International Journal of Modern Manufacturing Technologies
ISSN 2067–3604, Vol. X, No. 2 / 2018

FORWARD KINEMATICS AND NUMERICAL MODEL OF A FANUC AM100IB ROBOT

Adam Cholewa[1], Agnieszka Sekala[2], Jerzy Świder[3], Adrian Zbilski[4]

[1-4] Silesian University of Technology, Faculty of Mechanical Engineering, Konarskiego 18A, 44-100 Gliwice, Poland

Corresponding author: Jerzy Świder, jerzy.swider@polsl.pl

Abstract: The subject of this paper is focused on the verification of forward kinematics of a Fanuc AM100iB robot based on its numerical model, prepared in the form of a block diagram in Simulink software, using the SimMechanics toolbox. The main task of the numerical model of a Fanuc AM 100iB robot is to calculate the value of torques putting a load on motor shafts, and to calculate the values of kinematic parameters of the robot's arms in real time and in interactive mode. The developed kinematic model of the machine was verified using tests on an actual robot model. The values and format of torques putting a load on subsequent joints, and then on the motor shafts, resulted from the effect of the simultaneous action of all torques and the delay, resulting from the implementation of numerical calculations in real time.

Key words: industrial robot, numerical model, energy consumption, forward kinematics.

1. INTRODUCTION

Today's industrial robots have progressively become more and more sophisticated. Robots are increasingly replacing humans in monotonous work or work demanding extreme precision, not attainable for humans. The benefits of an increasing level of automation and robotics are noticeable in many industries due to the constantly increasing level of competitiveness, reducing production costs combined with an increase in the quality and reliability of products and services. Robotic production systems enable efficient use of both human resources as well as the machinery, thus contributing to an increase in production flexibility, improving the quality and quantity of production and environmental protection. The complexity and variety of components forming a part of robotic production cells causes that already at the stage of their design it becomes necessary to develop models depicting various aspects of their construction and operation. Advanced robotic manufacturing systems are an integral part of developing manufacturing companies, both those operating in the segment of small and medium-sized enterprises as well as large corporations. Robotic manufacturing systems enable efficient use of both human resources as well as the machinery, thus contributing to an increase in production flexibility, improving the quality and quantity of production and environmental protection. Designing robotic manufacturing cells forces the search for such engineering solutions, which will contribute in a maximum extent to the efficient use of machinery and equipment, as well as to the improvement of the energy-efficiency of the entire system. The complexity and variety of components forming a part of robotic production cells causes that already at the stage of their design it becomes necessary to develop models depicting various aspects of their construction and operation. Advanced robotic manufacturing systems are an integral part of developing manufacturing companies, both those operating in the segment of small and medium-sized enterprises as well as large corporations. Robotic manufacturing systems enable efficient use of both human resources as well as the machinery, thus contributing to an increase in production flexibility, improving the quality and quantity of production and environmental protection. Designing robotic manufacturing cells forces the search for such engineering solutions, which will contribute in a maximum extent to the efficient use of machinery and equipment, as well as to the improvement of the energy-efficiency of the entire system

2. FORWARD KINEMATICS

The subject of discussion is an industrial robot Fanuc AM 100iB with six degrees of freedom and spherical workspace. This article assumes orientations of the local coordinate systems as shown in Figure 1. The phenomenological model of a robot is presented in Figure 2. This system results from the directions of rotation adopted in the actual robot, and from the modified Denavit-Hartenberg notation (DH) [1-4, 7, 8]. The corresponding values of the DH parameters and listed in Table 1.

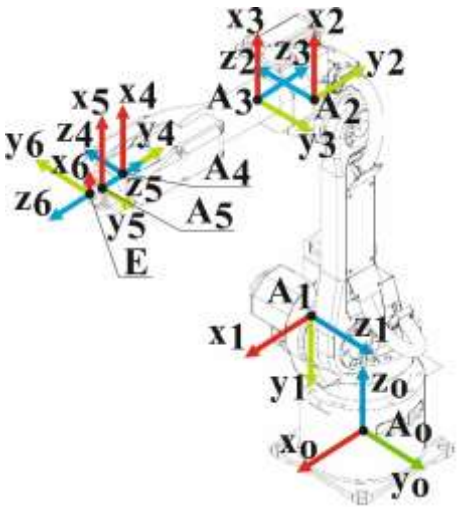

Fig. 1. Tested object

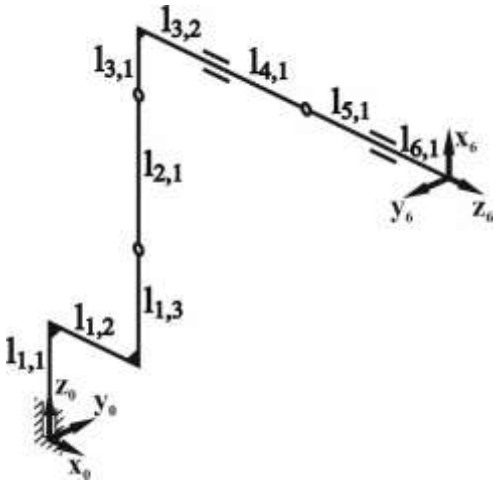

Fig. 2. A phenomenological model of the robot

Table 1. The Denavit-Hartenberg parameters [1, 5]

Nr	q_i	λ_i	l_i	α_i
1.	q_1	$l_{1,1}+l_{1,3}$	$l_{1,2}$	-90
2.	$\left(q_2-\frac{\pi}{2}\right)$	0	$l_{2,1}$	180
3.	q_3	0	l_{3,mod_1}	-90
4.	q_4	$-l_{4,1}$	0	90
5.	q_5	$-l_{5,1,\mathrm{mod}_2}$	0	-90
6.	q_6	$-l_{6,z}$	$\left[l_{6,x} \quad l_{6,y}\right]^T$	180

Rotation of axes

$$\mathrm{R}_{i-1}^{i}=\mathrm{Rot}_{i-1}^{i}(\mathrm{z}_{i-1},\mathrm{q}_i)\cdot\mathrm{Rot}_{i-1}^{i}(\mathrm{x}_i,\alpha_i) \tag{1}$$

The axis of rotation of joint 1:

$$\mathrm{R}_0^1=\mathrm{Rot}_0^1(\mathrm{z}_0,\mathrm{q}_1)\cdot\mathrm{Rot}_0^1(\mathrm{x}_1,\alpha_1) \tag{2}$$

$$\mathbf{R}_{\mathbf{0}}^{\mathbf{1}}=\begin{bmatrix} c(q_1) & 0 & -s(q_1) \\ s(q_1) & 0 & c(q_1) \\ 0 & -1 & 0 \end{bmatrix} \tag{3}$$

The axis of rotation of joint 2:

$$R_1^2=Rot_1^2(z_1,q_2-\frac{\pi}{2}) \tag{4}$$

$$\mathbf{R}_{\mathbf{1}}^{\mathbf{2}}=\begin{bmatrix} c\left(q_2-\frac{\pi}{2}\right) & s\left(q_1-\frac{\pi}{2}\right) & 0 \\ s\left(q_2-\frac{\pi}{2}\right) & -c\left(q_1-\frac{\pi}{2}\right) & 0 \\ 0 & 0 & -1 \end{bmatrix} \tag{5}$$

The axis of rotation of joint 3:

$$\mathrm{R}_2^3=\mathrm{Rot}_2^3(\mathrm{z}_2,\mathrm{q}_3)\cdot\mathrm{Rot}_2^3(\mathrm{x}_3,\alpha_3) \tag{6}$$

$$\mathbf{R}_{\mathbf{2}}^{\mathbf{3}}=\begin{bmatrix} c(q_3) & 0 & -s(q_3) \\ s(q_3) & 0 & c(q_3) \\ 0 & -1 & 0 \end{bmatrix} \tag{7}$$

The axis of rotation of joint 4:

$$\mathrm{R}_3^4=\mathrm{Rot}_3^4(\mathrm{z}_3,\mathrm{q}_4)\cdot\mathrm{Rot}_3^4(\mathrm{x}_4,\alpha_4) \tag{8}$$

$$\mathbf{R}_{\mathbf{3}}^{\mathbf{4}}=\begin{bmatrix} c(q_4) & 0 & s(q_4) \\ s(q_4) & 0 & -c(q_4) \\ 0 & 1 & 0 \end{bmatrix} \tag{9}$$

The axis of rotation of joint 5:

$$\mathrm{R}_4^5=\mathrm{Rot}_4^5(\mathrm{z}_4,\mathrm{q}_5)\cdot\mathrm{Rot}_4^5(\mathrm{x}_5,\alpha_5) \tag{10}$$

$$\mathbf{R}_{\mathbf{4}}^{\mathbf{5}}=\begin{bmatrix} c(q_5) & 0 & -s(q_5) \\ s(q_5) & 0 & c(q_5) \\ 0 & -1 & 0 \end{bmatrix} \tag{11}$$

The axis of rotation of joint 5:

$$\mathrm{R}_5^6=\mathrm{Rot}_5^6(\mathrm{z}_5,\mathrm{q}_6) \tag{12}$$

$$\mathbf{R}_5^6 = \begin{bmatrix} c(q_6) & s(q_6) & 0 \\ s(q_6) & -c(q_6) & 0 \\ 0 & 0 & -1 \end{bmatrix} \tag{13}$$

The general transformation matrix T_{i-1}^{i} a single link can be obtained as follows:

$$T_{i-1}^{i} = \mathrm{Rot}(z,q_i)\cdot\mathrm{Trans}(z\lambda_i)\cdot\mathrm{Trans}(x,l_i)\cdot\mathrm{Rot}(x,\alpha_i) \tag{14}$$

Transforming the first local coordinate system:

$$T_0^1 = \mathrm{Rot}(z_0,q_1)\cdot\mathrm{Trans}(0,0,\lambda_1)\cdot\mathrm{Trans}(l_{1,2},0,0)\cdot\mathrm{Rot}(x,\alpha_1) \tag{15}$$

$$T_0^1 = \left[\begin{array}{ccc|c} & R_0^1 & & \begin{matrix} c(q_1)\cdot l_{1,2} \\ s(q_1)\cdot l_{1,2} \\ l_{1,1}+l_{1,3} \end{matrix} \\ \hline 0 & 0 & 0 & 1 \end{array}\right] \tag{16}$$

Transforming the second local coordinate system:

$$T_1^2 = \mathrm{Rot}(z_1,q_2)\cdot\mathrm{Trans}(l_{2,1},0,0) \tag{17}$$

$$T_1^2 = \left[\begin{array}{ccc|c} & R_1^2 & & \begin{matrix} c\left(q_1-\frac{\pi}{2}\right)\cdot l_{2,1} \\ s\left(q_1-\frac{\pi}{2}\right)\cdot l_{2,1} \\ 0 \end{matrix} \\ \hline 0 & 0 & 0 & 1 \end{array}\right] \tag{18}$$

Transforming the third local coordinate system:

$$T_{2,\mathrm{mod}_1}^3 = \mathrm{Rot}(z_2,q_3)\cdot\mathrm{Trans}_{\mathrm{mod}_1}\left(-\sqrt{(l_{3,2})^2+(l_{3,1})^2},0,0\right)\cdot\mathrm{Rot}(x_3,\alpha_3) \tag{19}$$

$$T_{2,\mathrm{mod}_1}^3 = \left[\begin{array}{ccc|c} & R_2^3 & & \begin{matrix} -\cos\left[\left(q_3+\frac{\pi}{2}\right)+\mathrm{a\,tan}\left(\frac{l_{3,1}}{l_{3,2}}\right)\right]\cdot\sqrt{(l_{3,2})^2+(l_{3,1})^2} \\ -\sin\left[\left(q_3+\frac{\pi}{2}\right)+\mathrm{a\,tan}\left(\frac{l_{3,1}}{l_{3,2}}\right)\right]\cdot\sqrt{(l_{3,2})^2+(l_{3,1})^2} \\ 0 \end{matrix} \\ \hline 0 & 0 & 0 & 1 \end{array}\right] \tag{20}$$

The introduced modification mod_1 was responsible for the translation of the beginning of the third coordinate system exactly in place of the end of the third link, according to the equation 19. This translation was obtained by introducing an additional transformation that did not change the orientation of the transformed local coordinate system, only its location

Transforming the fourth local coordinate system:

$$T_3^4 = \mathrm{Rot}(z_3,q_4)\cdot\mathrm{Trans}(-l_{4,1},0,0)\cdot\mathrm{Rot}(x_4,\alpha_4) \tag{21}$$

$$T_3^4 = \left[\begin{array}{ccc|c} & R_3^4 & & \begin{matrix} 0 \\ 0 \\ -l_{4,1} \end{matrix} \\ \hline 0 & 0 & 0 & 1 \end{array}\right] \tag{22}$$

Transforming the fifth local coordinate system:

$$T_{4,\mathrm{mod}_2}^5 = \mathrm{Rot}(z_4,q_5)\cdot\mathrm{Rot}(x_5,\alpha_5)\cdot\mathrm{Trans}_{\mathrm{mod}_2}(0,0,l_{5,1}) \tag{23}$$

$$T_{4,\mathrm{mod}_2}^5 = \left[\begin{array}{ccc|c} & R_4^5 & & \begin{matrix} 0 \\ 0 \\ 0 \end{matrix} \\ \hline 0 & 0 & 0 & 1 \end{array}\right] \cdot \begin{bmatrix} 1 & 0 & 0 & 0 \\ 0 & 1 & 0 & 0 \\ 0 & 0 & 1 & -l_{5,1} \\ 0 & 0 & 0 & 1 \end{bmatrix} \tag{24}$$

The modification mod_2 separated rotation and translation operations by writing the translation of the fifth local coordinate system as the last operation (23). These operations performed in this order reproduced the position and orientation of the fifth local coordinate system in the numerical model.

Transforming the sixth local coordinate system:

$$T_5^6 = \mathrm{Rot}(z_5, q_6) \cdot \mathrm{Trans}(0,0,-l_{6,1}) \cdot \mathrm{Rot}(x_6, \alpha_6) \tag{25}$$

$$T_5^6 = \begin{bmatrix} & R_5^6 & & 0 \\ & & & 0 \\ & & & -l_{6,1} \\ 0 & 0 & 0 & 1 \end{bmatrix} \tag{26}$$

Based on the classical algorithm of the analysed notation, a kinematic model of the robot was developed in Matlab Simulink software. The model of the machine developed was verified using appropriate tests. The tests consisted in positioning the robot operating in the mode of controlling the values of natural angles in selected points of its workspace and reading the indications of the coordinate values of the TCP point in the robot's global coordinate system on the operator panel. Validation of the model consisted of entering the same values of natural angles that were used for positioning the robot in its inputs and calculating the coordinate values of the TCP of the machine's CAE model, and then comparing the results obtained with the values read (tables 2-5). In fact, several tests were conducted, and due to the fact that the number of pages of the article is limited - only selected experiments are presented in this paper.

Table 2. Validation of the kinematic model. Test No. 1

Set values					
J1	J2	J3	J4	J5	J6
60	-35	40	55	80	-45
Control system					
X		Y		Z	
24.980		204.608		1017.843	
CAE model of the robot					
X		Y		Z	
24.980		204.608		1017.843	

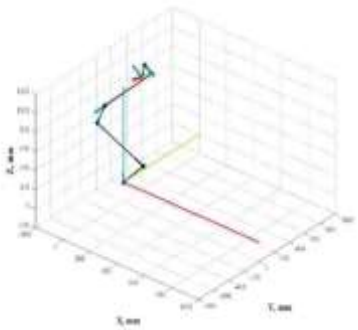

Table 3. Validation of the kinematic model. Test No. 2

Set values					
J1	J2	J3	J4	J5	J6
-60	60	-40	-55	80	135
Control system					
X		Y		Z	
660.865		-983.311		-73.143	
CAE model of the robot					
X		Y		Z	
660.865		-983.311		-73.143	

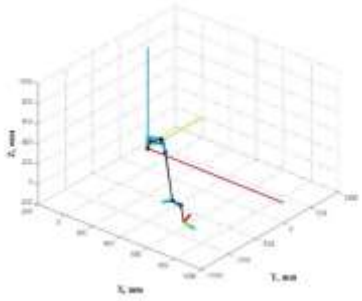

Table 4. Validation of the kinematic model. Test No. 3

Set values					
J1	J2	J3	J4	J5	J6
-60	-35	40	55	80	0
Control system					
X		Y		Z	
24.980		204.608		1017.843	
CAE model of the robot					
X		Y		Z	
24.980		204.608		1017.843	

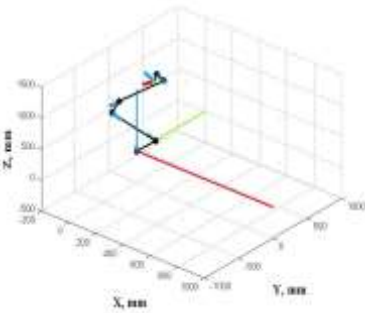

Table 5. Validation of the kinematic model. Test No. 4

Set values					
J1	J2	J3	J4	J5	J6
0	-35	0	55	0	0
Control system					
X		Y		Z	
520.854		0		591.491	
CAE model of the robot					
X		Y		Z	
520.854		0		591.491	

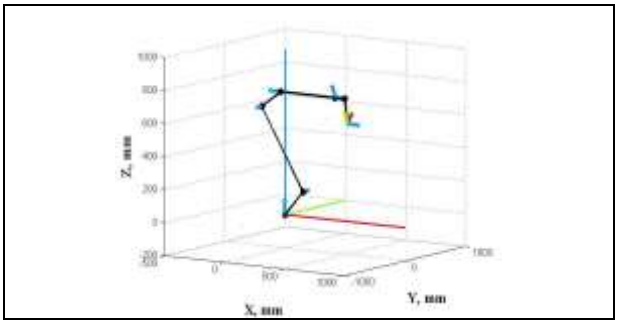

The input data for the model were the value of geometric parameters, obtained using their direct recording in the tested machine, during the execution of selected tasks. Using a numerical model, the behaviour of an actual machine was reconstructed.

Numerical calculations fully agree with the actual reading of coordinates and orientation of the robot manipulator's member in space. The developed numerical model was used to build a dynamic model of the analysed robot.

3. NUMERICAL MODEL OF FANUC AM 100IB

Numerical model of Fanuc AM 100iB robot was prepared in the form of a block diagram in Simulink software, using the SimMechanics toolbox. Relations between the members and the flow of input and output information is shown in Figure 3 [1, 6].

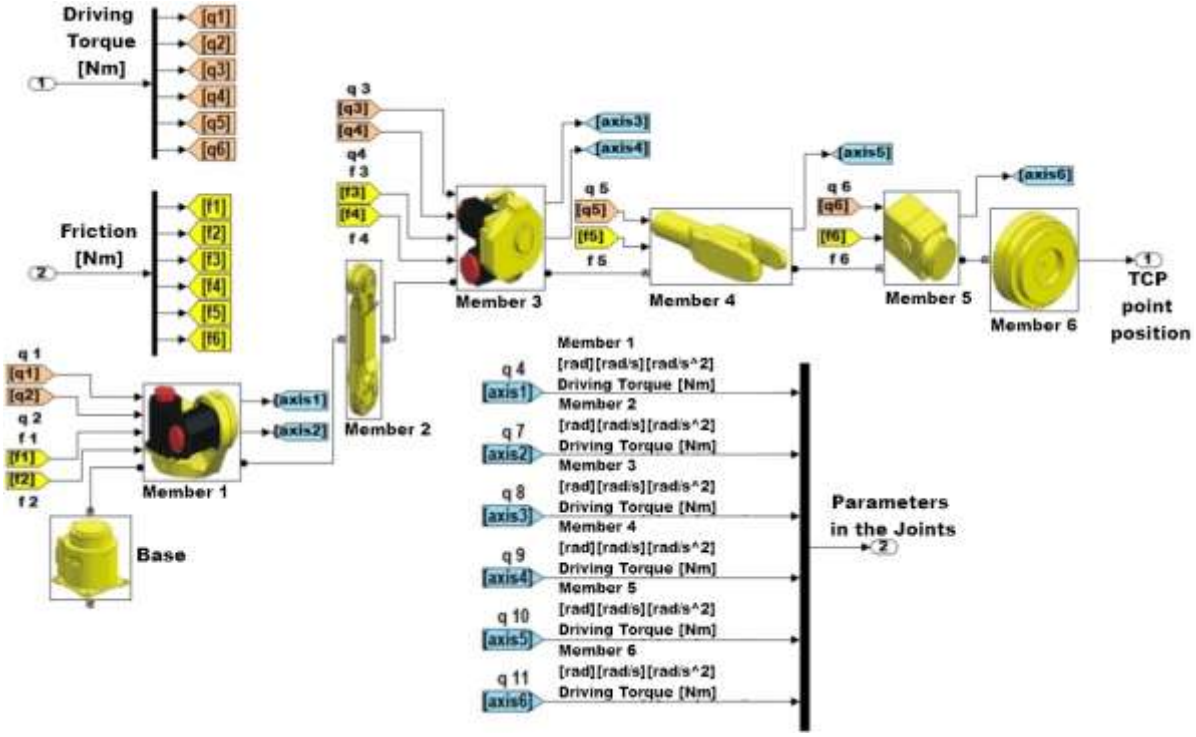

Fig. 3. The first layer of the block diagram of a numerical model of the robot

The input parameters were the values of driving torques - *Driving torque [Nm]*, achieved on the motor shafts, and the value of viscous friction on the joints - *Friction [Nm]*. The output values were the determined values of kinematic parameters of all members, and the achieved values of torques placing a load on motor shafts - *Parameters in the Joints*. An additional output parameter was a vector of the achieved coordinates of the position of the robot's TCP point, expressed in Cartesian coordinates - *TCP point position*. Model of the robot's base - *Base*, defined the value of components of the acceleration vector using the block - *Environment*, (Figure 4.).

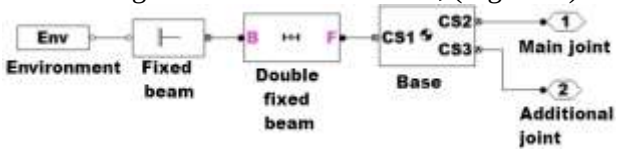

Fig. 4. Method of connecting the joints and members of the numerical model of the robot

This block also defined the resolution of calculations implemented. Blocks of the robot's members - *Member i* (Figure 5.), contain information about the values of dynamic parameters, which include the mass of members, the position of the centres of gravity of the robot's arms and their inertia tensors [1]. In addition, these blocks define the values of geometrical parameters, i.e. the length of the arms. Models of the robot's members and models of joints are grouped in a way that reflects the construction of an actual robot. Figure 4 also shows the connections between the members and the robot's joints. The same diagram is used to connect all the arms.

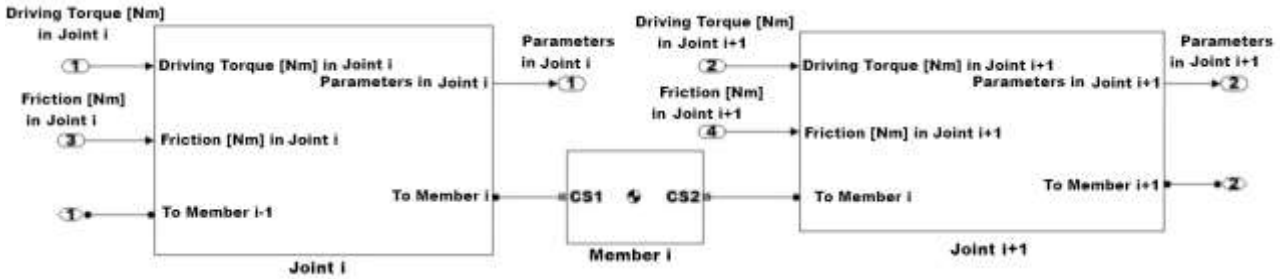

Fig. 5. Block diagram of the model of the robot's base

Block - *Joint* (Figure 5), contains information about the type of the kinematic pair with one degree of freedom - *Rotary kinematic pair*, which was identical in each joint (Figure 6). Block - *Mechanical Advantage of Joint i*, and block 1/*Mechanical Advantage of Joint i* (Figure 6), contain information about the values of the ratio and the inverse ratio of the mechanical advantage in the given joint.¶

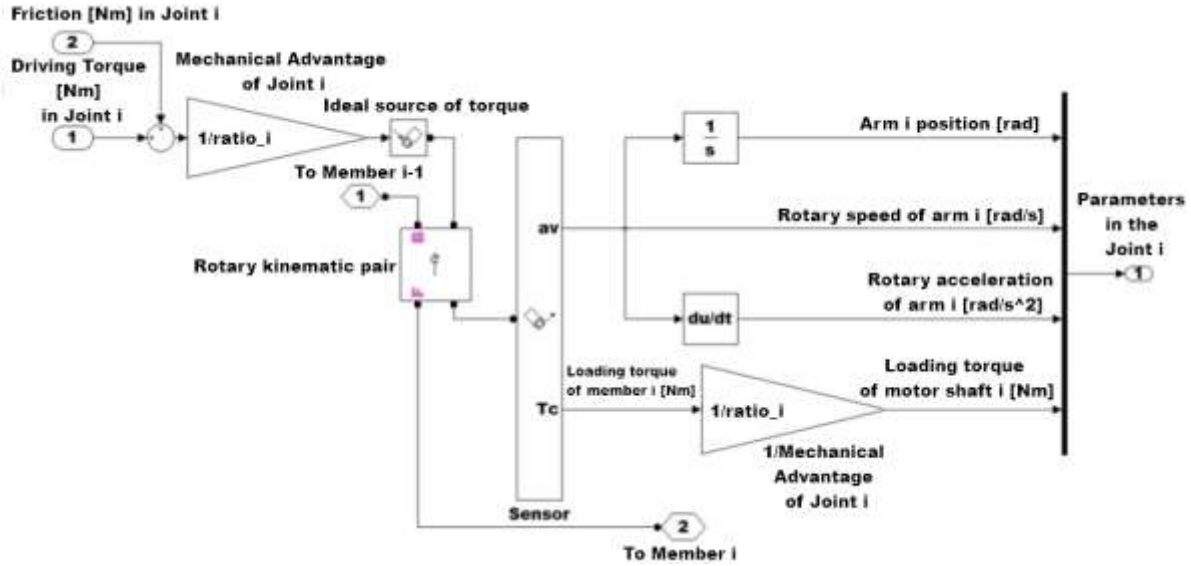

Fig. 6. Block diagram of the model of all of the robot's joints

Using the block - *Sensor*, a numerical measurement was performed of the implemented values of kinematic parameters of the rotation of the robot's members - *Arm i position [rad]* - *Rotary speed of arm i [rad/s]* - *Rotary acceleration of arm i [rad/s^2]* and the values of the torques putting a load on the members - *Loading torque of member i [Nm]*, reduced on the motor shafts - *Loading torque of motor shaft i [Nm]*. The effects of viscous friction were taken into account by algebraically adding its value to the value of the driving torque, expanded on each motor shaft. To generate the driving torque, a block of the ideal source of torque was used - *Ideal source of torque.* The value of the generated driving torque was calculated by means of a separate control system.

In the next stage, tests were conducted to confirm the consistency of the previously developed mathematical model with the real object. These tests were made possible thanks to the measuring equipment specially developed for this purpose. During the experiment, the respective axes of the robot were shifted in certain angular ranges of their movement. Table 1 lists the angular ranges of the working movement performed of each of the robot's arms.

Waveforms, describing the instantaneous angular positions of the shaft encoders of the motors in individual axes of the robot during the experiment, and the accompanying waveforms of voltages and currents are summarised in Figures 7-12.

Figure 6 shows the form of signals corresponding to the angular movements of the individual axes, waveforms of the intensities of currents and voltages recorded on the servo motors of individual axes registered for the configuration, in which the 1st, 3rd, 4th and 6th axis remain stationary, the 2nd axis moves from -35° to 60°, and the 5th axis moves in the range from 80° to -80°. Figure 7 shows the waveforms for a configuration in which the 1st, 3rd, 5th and 6th axis are stationary, the 2th axis moves in the range from -35° to 60°, and the 4th axis moves in the range of from 55° to -55°. The case shown in Figure 8 corresponds to the situation in which the 2nd axis is moved in the range from -35° to 60°, the 2rd axis in the range from 40° to -40° and the other axes do not move.

Table 5. Angular ranges of the working movement performed of each of the robot's arms

No	Axis 1 (J1)		Axis (J2)		Axis 3 (J3)		Axis 4 (J4)		Axis 5 (J5)		Axis 6 (J6)	
	Start [°]	Stop [°]	Start [°]	Stop [°]	Start [°]	Stop [°]	Start [°]	Stop [°]	Start [°]	Stop [°]	Start [°]	Stop [°]
1	60	-60	-35	60	40	-40	55	-55	80	-80	-45	135
2	60	-60	-35	60	40	-40	55	-55	80	-80	0	0
3	60	-60	-35	60	40	-40	55	-55	0	0	0	0
4	60	-60	-35	60	40	-40	0	0	0	0	0	0
5	60	-60	-35	60	0	0	0	0	0	0	0	0
6	60	-60	0	0	40	-40	0	0	0	0	0	0
7	60	-60	0	0	0	0	55	-55	0	0	0	0
8	60	-60	0	0	0	0	0	0	80	-80	0	0
9	0	0	-35	60	40	-40	0	0	0	0	0	0
10	0	0	-35	60	0	0	55	-55	0	0	0	0
11	0	0	-35	60	0	0	0	0	80	-80	0	0

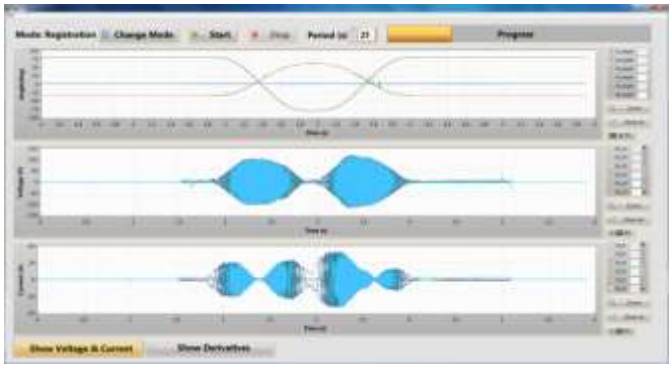

Fig. 7. 1st example of the recorded signal waveforms

The case shown in Figure 10 corresponds to the settings, in which the 1st axis is moved in the range from 60° to -60°, the 2nd axis in the range from -35° to 60° and the other axes do not move. In the case of rotation of the 1st axis in the range from 60° to -60°, the 2nd axis in the range from -35° to 60°, and the 4th axis in the range from 55° to -55°, waveforms as presented in Figure 10 were recorded. Figure 12 corresponds to the situation in which simultaneous rotation takes place in the 1st, 2nd and 3rd axes, respectively, in angular ranges of <60°, -60°>, <-35°, 60°> and <40°, -40°>.

The test performed allowed for correcting the values of the model's parameters.

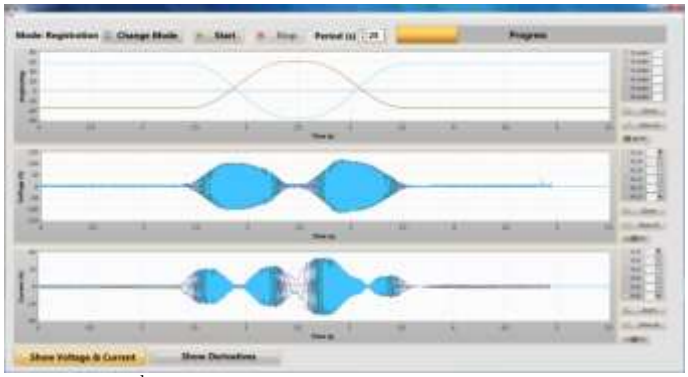

Fig. 8. 2nd example of the recorded signal waveforms

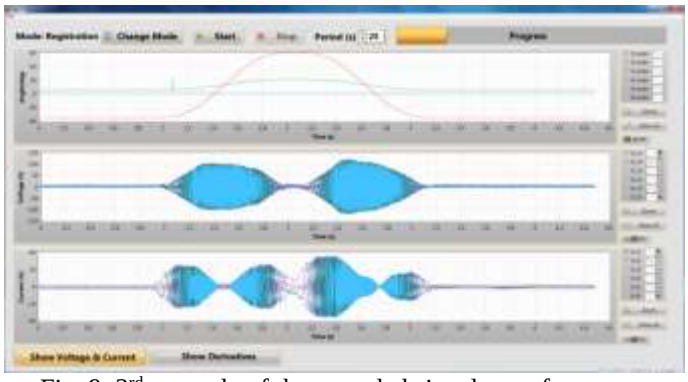

Fig. 9. 3rd example of the recorded signal waveforms

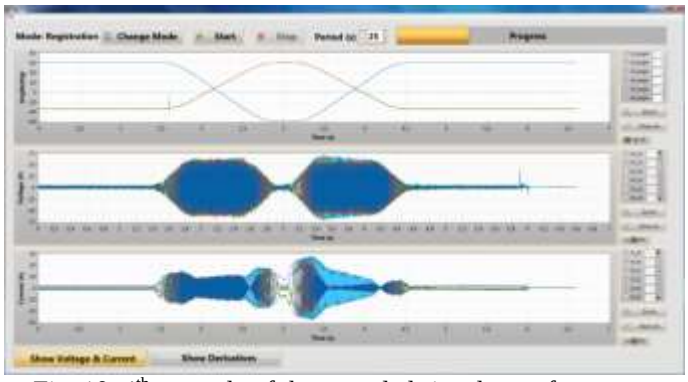

Fig. 10. 4th example of the recorded signal waveforms

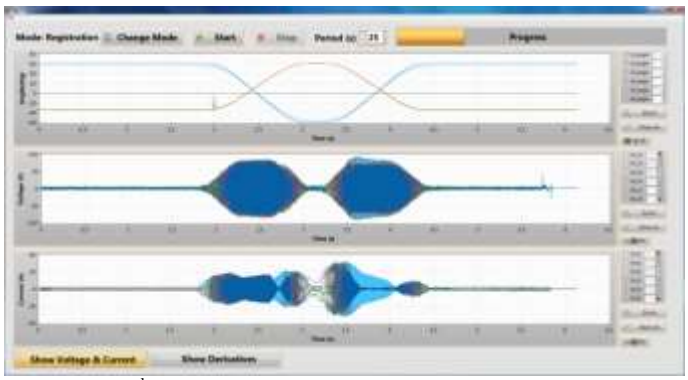

Fig. 11. 5th example of the recorded signal waveforms

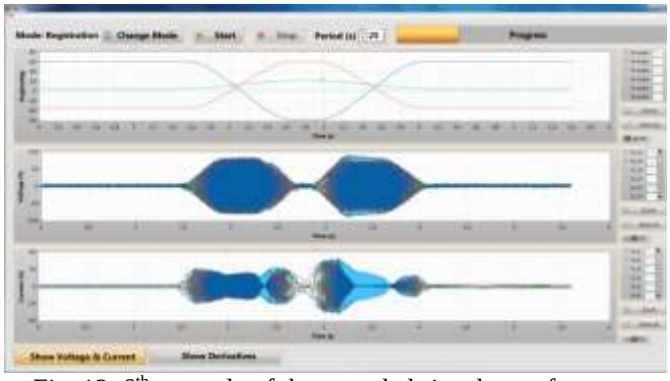

Fig. 12. 6th example of the recorded signal waveforms

4. CONCLUSIONS

The developed kinematic model of the machine was verified using tests on an actual robot model. The tests consisted in positioning the robot operating in the mode of controlling the values of natural angles in selected points of its workspace and reading the indications of the coordinate values of the TCP point in the robot's global coordinate system on the operator panel. Validation of the model consisted of entering the same values of natural angles that were used for positioning the robot in its inputs and calculating the coordinate values of the TCP of the machine's CAE model, and then comparing the results obtained with the values read. These results are the introduction to the partial verification of the dynamic model of the analysed device.

The input data for the model were the value of kinematic parameters, obtained using their direct recording in the tested machine, during the execution of selected tasks. The numerical model has also been supplemented by the approximately identified values of dynamic parameters, which were verified by measurements carried out using measurement equipment. The developed numerical model of the robot should be supplemented with a system controlling the orientation of the robot's member. In conjunction with existing systems, this will enable carrying out further research on the development of methods for generating, for example, energy-efficient trajectories.

5. ACKNOWLEDGMENTS

The project was financed from the funds of National Science Centre awarded on the basis of a decision number DEC-2011/03/B/ST8/04631.

6. REFERENCES

1. Świder, J., Cholewa, A., Zbilski, A., (2015). *Computer aided analysis of energy consumtion in the Fanuc AM100iB robot drives during manipulation and transportation processes*., Monograph. (Publisher: Wydawnictwo Pracowni Komputerowej Jacka Skalmierskiego, Gliwice (in polish)), Gliwice.

2. Zbilski, A., (2014). *Method for energy intensity analysis of manipulation and transportation processes*. Doctoral dissertation, Silesian University of Technology (in polish).

3. Świder, J., Zbilski, A., (2013). *The modelling and analysis of a partial loads in the Fanuc AM100iB robot joints*. International Journal of Modern Manufacturing Technologies, 2, 89-96.

4. Świder, J., Zbilski, A., (2013). *Modelling of the power of losses in the Fanuc AM100iB robot drives and in its power electronic systems*. Modelowanie inzynierskie - Engineering modeling, 1748, 138-142.

5. Craig J. (2005) *Introduction to Robotics Mechanics and Contro*l, 3rd Edition, Pearson Prentice Hall, Upper Saddle River, pp. 62-100.

6. Cholewa, A., Świder, J., Zbilski, A., (2016). *Numerical model of Fanuc AM100iB robot*. IOP Conf. Ser.: Mater. Sci. Eng. 145, 052002.

7. Cholewa, A., Świder, J., Zbilski, A., (2016). *Verification of forward kinematics of the numerical and analytical model of Fanuc AM100iB robot*. IOP Conf. Ser.: Mater. Sci. Eng. 145, 052001.

8. Płaczek, M., Piszczek, Ł., (2018). *Testing of an industrial robot's accuracy and repeatability in off and online environment*. Eksploatacja i Niezawodnosc – Maintenance and Reliability, 20 (3), 455–464, http://dx.doi.org/10.17531/ein.2018.3.15.

Received: June 11, 2018 / Accepted: December 15, 2018 / Paper available online: December 20, 2018